

ac susceptibility and magnetic relaxation of $R_2\text{PdSi}_3$ ($R=\text{Nd, Tb, and Dy}$)D. X. Li,¹ S. Nimori,² Y. Shiokawa,¹ Y. Haga,³ E. Yamamoto,³ and Y. Onuki³¹*Institute for Materials Research, Tohoku University, Oarai, Ibaraki, 311-1313 Japan*²*Tsukuba Magnet Laboratory, National Research Institute for Materials Science, 3-13 Sakura, Tsukuba, 305-0003 Japan*³*Advanced Science Research Center, Japan Atomic Energy Research Institute, Tokai, Ibaraki, 319-1195 Japan*

(Received 3 December 2002; revised manuscript received 24 April 2003; published 30 July 2003)

The results of ac susceptibility and magnetic relaxation measurements on $R_2\text{PdSi}_3$ ($R=\text{Nd, Tb, and Dy}$), a class of compounds previously shown in the literature to exhibit interesting properties, are reported. The data for the Nd compound show spin-glass-like anomalies at the temperature where long-range ferromagnetic ordering sets in. While we observed two magnetic transitions for Tb and Dy compounds in agreement with the literature, the ones occurring at the lower temperature side is shown to exhibit spin-glass-like anomalies. These results are compared with those reported for other 2:1:3 compounds.

DOI: 10.1103/PhysRevB.68.012413

PACS number(s): 75.50.Lk, 75.50.Ee, 75.50.Gg

Nonmagnetic atom disorder (NMAD) ternary intermetallic compounds with the composition R_2MX_3 ($R=\text{rare earth or U, } M=\text{transition metals, } X=\text{Si or Ge}$) became a subject of intensive studies during the last few years. Among them $R_3\text{PdSi}_3$, crystallizing in an AlB_2 -derived hexagonal structure with random distribution of Pd and Si atoms in the B network, is a very interesting series exhibiting unusual magnetic and transport behaviors as recently revealed by the neutron diffraction,¹ dc magnetization,¹⁻⁴ electrical resistivity,¹⁻⁴ and specific heat² measurements. Compounds Nd_2PdSi_3 , Tb_2PdSi_3 , and Dy_2PdSi_3 are the typical examples in this series relevant to their characteristic spin structures. Neutron diffraction results¹ establish that the ordering of magnetic moments in these compounds varies from simple ferromagnetism in Nd_2PdSi_3 to a ferromagnetic spiral in Tb_2PdSi_3 and to a sinusoidally modulated structure in Dy_2PdSi_3 . A long-range magnetic ordering occurs at a temperature $T_0=17, 25,$ and 7.5 K for Nd_2PdSi_3 , Tb_2PdSi_3 , and Dy_2PdSi_3 , respectively, which was further confirmed by a specific heat peak² and a resistivity anomaly¹⁻⁴ at respective magnetic transition temperatures. All of them, both polycrystalline and single crystalline samples, show the magnetic history-dependent feature at low temperatures.^{1,3,4} In particular, a “two-peak structure” in temperature dependence of dc magnetization of Tb_2PdSi_3 was observed in low magnetic fields.^{1,3} For Dy_2PdSi_3 , the magnetization curve shows an evident increase with decreasing the temperature near 2 K,⁴ the lowest temperature measured, suggesting the second peak similar to that observed for Tb_2PdSi_3 might appear at much lower temperature. It has been clarified that the first peak on the high-temperature side is indicative of a long-range magnetic phase transition. Considering the existence of random distribution of Pd and Si atoms and the possible competing magnetic exchange interactions, we guess that the spin-glass (SG) mechanism may be responsible for the second peak at lower temperature side in Tb_2PdSi_3 , and similar anomaly could also exist in Dy or other $R_2\text{PdSi}_3$ compounds. In fact, the existence of a SG state (about 25% of the magnetic moment) in Tb_2PdSi_3 has been confirmed by neutron-diffraction measurement.¹ As further evidence for the formation of the SG state, in this paper we present the new results

of ac susceptibility and magnetic relaxation measurements on the three typical compounds.

The polycrystalline samples of Nd_2PdSi_3 , Tb_2PdSi_3 , and Dy_2PdSi_3 were prepared by melting appropriate amounts of the constituent elements in an arc furnace under purified argon atmosphere. The sample was then wrapped into tantalum foil and annealed in evacuated silica tube at 750 °C for 10 days. X-ray powder diffraction was performed at room temperature with Cu K_α radiation. The diffraction lines can be indexed based on the disordered hexagonal AlB_2 -type structure model (space group $P6/mmm$) with R atoms on $1a$ sites and Pd and Si atoms statistically distributed over the $2d$ sites. The determined room-temperature lattice constants are $a=4.105, 4.065,$ and 4.062 Å and $c=4.204, 4.052,$ and 4.031 Å for Nd_2PdSi_3 , Tb_2PdSi_3 , and Dy_2PdSi_3 , respectively. The ac susceptibility $\chi_{ac}(T)$ at various frequencies and magnetic relaxation $M(t)$ at different temperatures were measured using a Quantum Design superconducting quantum interference device (SQUID) magnetometer.

Figure 1 shows the in-phase $\chi'_{ac}(T, \omega)$ as well as the out-of-phase $\chi''_{ac}(T, \omega)$ components of the ac susceptibility versus temperature for Nd_2PdSi_3 , Tb_2PdSi_3 , and Dy_2PdSi_3 taken at frequency range $0.1 \text{ Hz} \leq \omega/2\pi \leq 1000 \text{ Hz}$. The features of the three samples are distinctly different. For Nd_2PdSi_3 , both χ'_{ac} and χ''_{ac} exhibit the characteristic pronounced maximums near $T_0=14.5$ K. As confirmed by the neutron diffraction and electrical resistivity measurements,¹ the resulting maximums in χ'_{ac} and χ''_{ac} are mainly ascribed to the long-range ferromagnetic phase transition. However, in contrast to a general ferromagnet, the position of the maximum shifts to higher temperature with increasing frequency ω for both χ'_{ac} and χ''_{ac} similar to that observed for a metastable SG system.⁵ Considering this frequency shift of peak position of ac susceptibility occurs at such low frequency values Nd_2PdSi_3 could not be considered as a simple ferromagnet, some influences originated from spin freezing may be in existence in this system to a certain extent.

On the other hand, Tb_2PdSi_3 shows a “two-peak structure” both in χ'_{ac} and χ''_{ac} curves. With decreasing the temperature, the first peak in χ''_{ac} appeared on the high-temperature side has a large amplitude. Note that such a peak

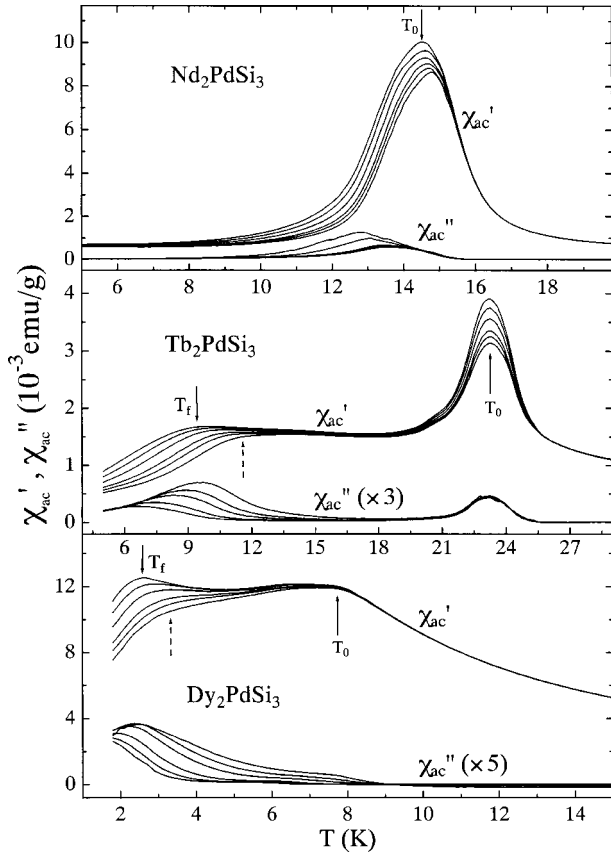


FIG. 1. Real (χ'_{ac}) and imaginary (χ''_{ac}) components of the ac susceptibility of R_2PdSi_3 vs temperature at various frequencies. The curves from left to right were measured at a frequency of 0.1, 1, 10, 100, 300, and 1000 Hz, respectively. T_0 and T_f represent the long-range magnetic ordering temperature and spin freezing temperature, respectively, defined as the peak (kink) position in χ'_{ac} ($\omega/2\pi=0.1$ Hz) curve (see the text).

in χ''_{ac} is absent in an antiferromagnetic system at Néel temperature. In addition, the peak position T_0 both in χ'_{ac} and χ''_{ac} is independent of ω . These properties suggest that the natures of χ'_{ac} and χ''_{ac} of Tb_2PdSi_3 around T_0 are mainly dominated by long-range ferromagnetic interactions. This is in agreement with the neutron diffraction and dc magnetization measurements, the former revealed a magnetic ordering with the ferromagnetic spiral type in this compound at T_0 ,¹ and the latter shows a large divergence between zero-field-cooled (ZFC) and field-cooled (FC) curves^{1,3} setting in at T_0 presumably due to domain-wall pinning effect. The ordering temperature determined as the peak position of χ'_{ac} to be $T_0=23.3$ K for our Tb_2PdSi_3 sample. Upon further decreasing T , both χ'_{ac} and χ''_{ac} display the second peaks (shoulders). The peak positions [$T_f(\omega)$] shift evidently to high temperatures with increasing ω suggesting the formation of a SG-like state.⁵ For a SG system, the spin freezing temperature T_f is a function of ω and H , and is generally defined as the peak temperature of χ'_{ac} in ac susceptibility. Using this method, T_f of Tb_2PdSi_3 is determined to be 9.6 K at $\omega/2\pi=0.1$ Hz.

In the case of Dy_2PdSi_3 , similar “two-peak structure” is evidently observed in χ'_{ac} curve alone. At high temperature

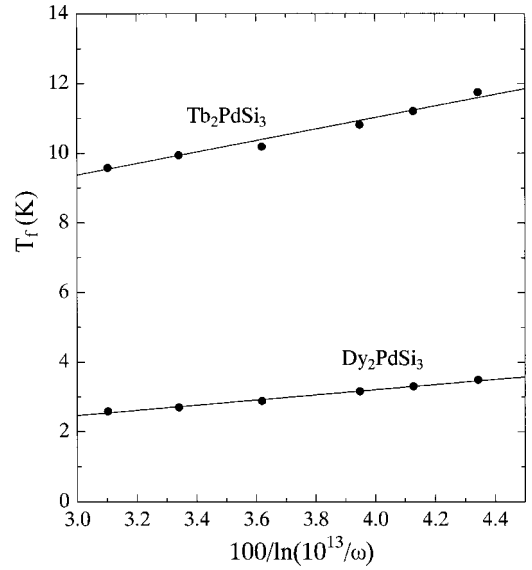


FIG. 2. T_f vs $1/\ln(\omega/\omega_0)$ plot for Tb_2PdSi_3 and Dy_2PdSi_3 with $\omega_0=10^{13}$ Hz. The solid lines represent the fits to the Vogel-Fulcher law.

side, χ'_{ac} exhibits a clear kink with amplitude and position (T_0) independent of ω , while there is no pronounced anomaly in χ''_{ac} curve around T_0 . We have also noted that the dc magnetization measurements^{1,4} show an obvious peak both in FC and ZFC curves at T_0 and the divergence of them is rather weak below and near T_0 . These features are different from those observed for Nd and Tb compounds indicating the dominant long-range antiferromagnetic interaction in Dy_2PdSi_3 around T_0 . The ordering temperature $T_0=7.7$ K is determined as the kink position in $\chi'_{ac}(T)$ curve. Similar to that observed for Tb_2PdSi_3 , the lower temperature side peak (shoulder) is evident for both χ'_{ac} and χ''_{ac} curves. The clear upward-shift of the peak position with increasing ω suggests the formation of a SG-like state. The spin freezing temperature defined as the peak position of χ'_{ac} curve to be $T_f=2.6$ K at $\omega/2\pi=0.1$ Hz.

ac susceptibility is very important for the investigation of SG behavior, which could offer a good criterion for distinguishing a canonical SG from a SG-like material.⁵ We are interested in the second peak in χ'_{ac} and χ''_{ac} observed on the lower-temperature side for Tb_2PdSi_3 and Dy_2PdSi_3 . In spin glasses (SG's), a criterion, namely, $\delta T_f = \Delta T_f / (T_f \Delta \ln \omega)$, has often been used for comparing the ω dependence of T_f in different systems. We find $\delta T_f=0.046$ for Tb_2PdSi_3 and $\delta T_f=0.044$ for Dy_2PdSi_3 . These values are comparable to those reported for other typical concentrated SG systems,⁵ e.g., (LaGd)Al₂: 0.060, (EuSr)S: 0.060, and some NMAD concentrated spin glasses, e.g., URh₂Ge₂: 0.025 (Ref. 6), Ce₂AgIn₃: 0.022 (Ref. 7), and U₂PdSi₃: 0.020 (Ref. 8). It should be emphasized that the value of T_f at high frequency used for calculating δT_f of Tb_2PdSi_3 and Dy_2PdSi_3 is determined as the temperature just below where χ'_{ac} decreases rapidly (for example, see the broken line arrow shown in Fig. 2 for curve of $\omega/2\pi=1000$ Hz). In fact, in contrast to canonical SG's, the second anomaly in χ'_{ac} is rather broad and there

is no definite peak in the high-frequency curves for both Tb and Dy compounds. In the case of Tb_2PdSi_3 , if T_f is determined from the centrepoint of the very broad shoulder in χ'_{ac} , one then arrives at a value of about 13.8 K for T_f at $\omega/2\pi=1000$ Hz and a value for δT_f greater than 0.1, much larger than what is observed in canonical SG's.⁵ For these reasons, we call the low- T anomaly observed in Tb_2PdSi_3 and Dy_2PdSi_3 "SG-like" transition. In the case of Nd_2PdSi_3 , although there also exists an upward-shift of the peak position in $\chi'_{ac}(\omega, T)$ and $\chi''_{ac}(\omega, T)$ with increasing ω , the initial frequency shift δT_0 calculated as $\delta T_0 = \Delta T_0 / (T_0 \Delta \ln \omega) = 0.006$ is much smaller than δT_f obtained for Tb_2PdSi_3 , Dy_2PdSi_3 , and other typical NMAD SG's. Even so we cannot negate this frequency shift having its origin in SG-like spin freezing in spite of the very small value of δT_0 , because the frequency shift of ac susceptibility peak position is a characteristic feature of SG behavior. Very similar magnetic properties have also been found for the isostructural compound Nd_2PtSi_3 (Ref. 9).

A better description of the frequency dependence of freezing temperature T_f of a SG can be obtained using the empirical Vogel-Fulcher law^{5,10}

$$\omega = \omega_0 \exp[-E_a/k_B(T_f - T_a)], \quad (1)$$

with three fitting parameters: characteristic frequency ω_0 , activation energy E_a (k_B is the Boltzmann constant), and Vogel-Fulcher temperature T_a . In other words, the freezing temperature T_f of a SG should be in proportion to $1/\ln(\omega_0/\omega)$. When $\omega_0/2\pi$ is 10^{13} Hz typically taken in the SG systems,¹¹ a linear variation of T_f (the temperature just below where χ'_{ac} decreases rapidly) versus $1/\ln(\omega_0/\omega)$ is also obtained for the Tb_2PdSi_3 and Dy_2PdSi_3 samples as illustrated in Fig. 2. The best fits of Eq. (1) to the experimental data yield the values of fitting parameters $E_a/k_B=165.17$ and 74.45 K and $T_a=4.42$ and 0.23 K for Tb_2PdSi_3 and Dy_2PdSi_3 , respectively. Clearly, the activation energies in Tb_2PdSi_3 and Dy_2PdSi_3 estimated in this method are $E_a = 17.2 k_B T_f$ for Tb_2PdSi_3 and $E_a = 28.6 k_B T_f$ for Dy_2PdSi_3 .

For a SG, the frequency-dependent ac susceptibility indicates the nonequilibrium characters of the low-temperature SG states. Thermodynamically, such nonequilibrium states directly relate to slow relaxation. The magnetic relaxations were studied at the temperatures below T_0 for Nd_2PdSi_3 and below T_f for Tb_2PdSi_3 and Dy_2PdSi_3 . In the insets of Fig. 3, we present the data of $M(t)/M(0)$ as a function of time t in a magnetic field much larger than the coercive field H_C .¹² The sample was first cooled in zero field from 200 K to the desired temperature, then a magnetic field (of 0.5 kOe for Nd_2PdSi_3 , 8.0 kOe for Tb_2PdSi_3 and 0.2 kOe for Dy_2PdSi_3) was applied and the measurement started at $t=0$ just as the field stabilized. The important finding is that long-time magnetic relaxation effects are clearly observed in these samples even in a field much larger than H_C . Magnetic relaxations of R_2PdSi_3 were also studied by measuring the isothermal remanent magnetization $M_{\text{IRM}}(t)$ as a function of t at low temperatures. First, we cooled the sample in zero field from 200 K to the desired temperature, then a magnetic field of 5.0 kOe was applied for 5 min and switched off at $t=0$. As

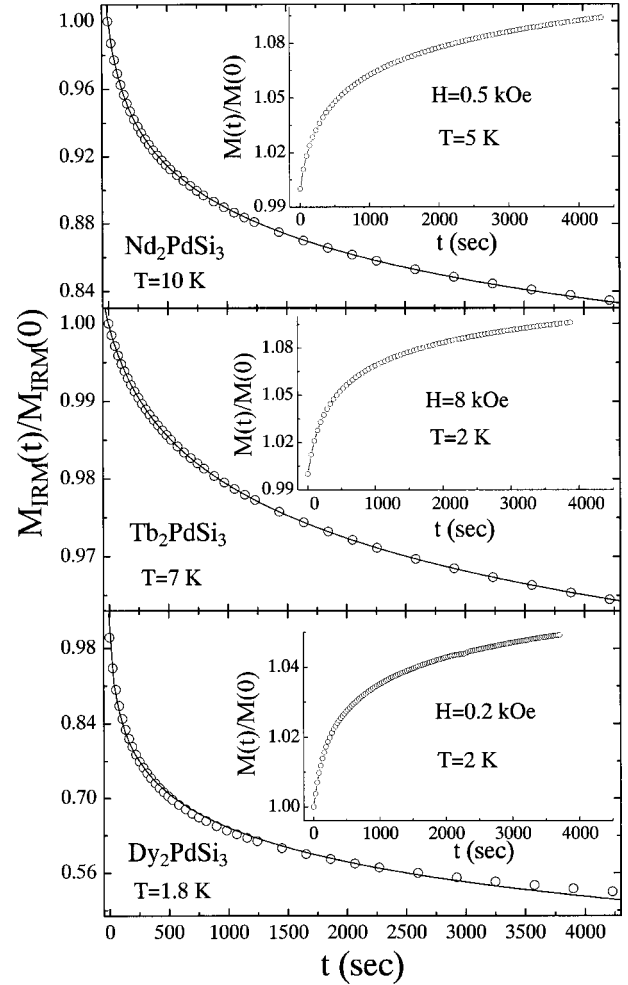


FIG. 3. Isothermal remanent magnetization $M_{\text{IRM}}(t)$ as a function of time t at 10, 7, and 1.8 K for Nd_2PdSi_3 , Tb_2PdSi_3 , and Dy_2PdSi_3 , respectively, plotted as $M_{\text{IRM}}(t)/M_{\text{IRM}}(0)$ vs t . The solid lines represent least-squares fits using equation $M_{\text{IRM}}(t) = M_0 - S \ln(1 + t/t_0)$. The insets show the data of $M(t)/M(0)$ as a function of t measured in a magnetic field much larger than the coercive field H_C (Ref. 12).

shown in Fig. 3, the decay of $M_{\text{IRM}}(t)$ is remarkably slow, after waiting for one hour, a nonzero remanence can also be observed.

The relaxation behavior of $M_{\text{IRM}}(t)$ showed in Fig. 3 for Nd_2PdSi_3 , Tb_2PdSi_3 , and Dy_2PdSi_3 could be fitted to a logarithmic function

$$M_{\text{IRM}}(t) = M_0 - S \ln(1 + t/t_0). \quad (2)$$

The same logarithmic function had also been used to describe the relaxation behavior of M_{IRM} for the isostructural $\text{Gd}_{2-x}\text{Y}_x\text{PdSi}_3$ ($x=0, 0.4, 1.0, \text{ and } 1.6$),¹³ where M_0 and S , called the initial zero-field magnetization and magnetic viscosity, respectively, are the fitting parameters depending on the temperature. The parameter t_0 depends on the measuring conditions and has only limited physical relevance.¹³ The best fitting results obtained by using the least-squares method are shown by the solid lines in Fig. 3 with $M_0 = 0.8359, 0.9649, \text{ and } 0.5309$ emu/g, and $S = 0.0332, 0.0108,$

and 0.0492 emu/g for Nd_2PdSi_3 , Tb_2PdSi_3 , and Dy_2PdSi_3 , respectively. It is emphasized that the characteristic phenomena of remanence and magnetic relaxation on macroscopic time scale can be observed for all SG's (Refs. 5 and 10) and for ferromagnet with high magnetic anisotropy.¹⁴ The long-time magnetic relaxation effect seems to have its main origin in spin freezing in Dy_2PdSi_3 , whereas, both the domain-wall pinning and spin freezing could contribute to this effect in Nd_2PdSi_3 and Tb_2PdSi_3 .

In a previous paper,⁹ we discussed that the necessary conditions, frustration and randomness, for the formation of SG state are possible in 2:1:3 NMAD systems. Among these compounds, long-range magnetic ordering may occur in some systems with strong magnetic exchange interactions such as in ferromagnets Nd_2PtSi_3 (Ref. 9) and Nd_2RhSi_3 (Ref. 15) and in antiferromagnets Tb_2RhSi_3 (Ref. 15) and Tb_2AgIn_3 .¹⁶ In contrast, for compounds with weak magnetic coupling SG state may dominate the magnetic properties such as in Ce_2AgIn_3 ,⁷ Ce_2CuSi_3 ,¹⁷ and some U_2MSi_3 compounds.⁸ In some cases both long-range magnetic ordering and SG states could coexist behaving as the reentrant SG characters such as in Tb_2CuIn_3 (Ref. 18) and Nd_2CuSi_3 .¹⁹ The present work confirms that reentrant SG-like features also exist in Tb_2PdSi_3 and Dy_2PdSi_3 . Very recently, interesting results were reported for an isostructural compound Ce_2PdSi_3 exhibiting reentrant magnetic feature.²⁰ According

to this report, in this Ce compound, there is one long-range magnetic transition around 4 K and the other one that is a SG-like below about 2 K, similar to that observed for Tb_2PdSi_3 and Dy_2PdSi_3 . It seems that in such reentrant SG-like systems a part of spins could exist as random individual spins or finite-size granules with net magnetic moments (magnetic clusters) due to the NMAD structure and do not participate in long-range magnetic ordering. As the temperature is further decreased down to a critical point T_f , these spins or clusters could weakly correlate with each other mediated by the conduction electrons and freeze into a SG-like state.

In summary the ac susceptibility and magnetic relaxation measurements give evidence for the formation of a SG-like state in Tb_2PdSi_3 and Dy_2PdSi_3 at low temperatures ($T_f = 9.6$ and 2.6 K, respectively) and SG-like behavior in Nd_2PdSi_3 at the temperature ($T_0 = 14.5$ K) where long-range magnetic ordering occurs. The SG-like phase in Tb_2PdSi_3 and Dy_2PdSi_3 is of reentrant character, which develops from a long-range ferromagnetic interaction dominated (ferromagnetic spiral) state for the former and from a long-range antiferromagnetic interaction dominated (sinusoidally modulated) state for the latter.

This work was supported by a Grant-in-Aid for Scientific Research (Grant No. 13640348) from the Ministry of Education, Culture, Sports, Science and Technology, Japan.

-
- ¹A. Szytula, M. Hofmann, B. Penc, M. Slaski, S. Majumdar, E. V. Sampathkumaran, and A. Zygmunt, *J. Magn. Magn. Mater.* **202**, 365 (1999).
- ²R. Mallik, E. V. Sampathkumaran, and P. L. Paulose, *Solid State Commun.* **106**, 169 (1998).
- ³S. Majumdar, E. V. Sampathkumaran, and P. L. Paulose, *Phys. Rev. B* **62**, 14 207 (2000).
- ⁴S. Majumdar, H. Bitterlich, G. Behr, W. Löser, P. L. Paulose, and E. V. Sampathkumaran, *Phys. Rev. B* **64**, 012418 (2001).
- ⁵J. A. Mydosh, *Spin Glass: An Experimental Introduction* (Taylor & Francis, London, 1993).
- ⁶S. Süllow, G. J. Nieuwenhuys, A. A. Menovsky, J. A. Mydosh, S. A. M. Mentink, T. E. Mason, and W. J. L. Buyers, *Phys. Rev. Lett.* **78**, 354 (1997).
- ⁷T. Nishioka, Y. Tabata, T. Taniguchi, and Y. Miyako, *J. Phys. Soc. Jpn.* **69**, 1012 (2000).
- ⁸D. X. Li, Y. Shiokawa, Y. Haga, E. Yamamoto, and Y. Onuki, *J. Phys. Soc. Jpn.* **71**, 418 (2002), and references therein.
- ⁹D. X. Li, S. Nimori, Y. Shiokawa, Y. Haga, E. Yamamoto, and Y. Onuki, *Solid State Commun.* **120**, 227 (2001).
- ¹⁰K. Binder and A. P. Young, *Rev. Mod. Phys.* **58**, 801 (1986).
- ¹¹For examples, see J. J. Prejean, *J. Phys. (France)* **39**, C6-907 (1978); J. L. Tholence, *Solid State Commun.* **35**, 113 (1980); J. Dho, W. S. Kim, and N. H. Hur, *Phys. Rev. Lett.* **89**, 027202 (2002); V. H. Tran, A. J. Zaleski, R. Troc, and P. de V. du Plessis, *J. Magn. Magn. Mater.* **162**, 247 (1996).
- ¹²In this work, the coercive field is determined to be 150 Oe for Nd_2PdSi_3 (at 5 K), 5.4 kOe for Tb_2PdSi_3 (at 2 K), and 50 Oe for Dy_2PdSi_3 (at 2 K) from the carefully measured hysteresis loops.
- ¹³S. Majumdar, E. V. Sampathkumaran, D. Eckert, A. Handstein, K. H. Müller, S. R. Saha, H. Sugawara, and H. Sato, *J. Phys.: Condens. Matter* **11**, L329 (1999), and references therein.
- ¹⁴R. Street and S. D. Brown, *J. Appl. Phys.* **76**, 6386 (1994).
- ¹⁵A. Szytula, J. Leciejewicz, and K. Maletka, *J. Magn. Magn. Mater.* **118**, 302 (1993).
- ¹⁶J. P. Semitelou, J. Siouris, J. K. Yakinthos, W. Schäfer, and D. Schmitt, *J. Alloys Compd.* **283**, 12 (1999).
- ¹⁷D. X. Li, Y. Shiokawa, S. Nimori, Y. Haga, E. Yamamoto, T. D. Matsuda, and Y. Onuki, *Physica B* (to be published).
- ¹⁸I. M. Siouris, I. P. Semitelou, J. K. Yakinthos, W. Schäfer, and R. Arons, *J. Alloys Compd.* **314**, 1 (2001).
- ¹⁹C. Tien and L. Luo, *Solid State Commun.* **107**, 295 (1998).
- ²⁰E. V. Sampathkumaran, cond-mat/0207447 (unpublished), and references therein.